Influence Mechanism of Process Parameters on Nanosecond Laser Polishing Quality of Ti6Al4V Titanium Alloy

Xulin Wang * and Jianwei Ma

Posted Date: 2 February 2026

doi: 10.20944/preprints202602.0092.v1

Keywords: Ti6Al4V titanium alloy; nanosecond laser; surface roughness; polishing quality; physical mechanism

 doi:10.20944/preprints202602.0092.v1

Article

Influence Mechanism of Process Parameters on Nanosecond Laser Polishing Quality of Ti6Al4V Titanium Alloy

Xulin Wang [1,*] and Jianwei Ma [2]

[1] School of General Aviation and Flight, Nanjing University of Aeronautics and Astronautics, Liyang 213300, China

[2] School of Mechanical Engineering, Dalian University of Technology, Dalian 116024, China

* Correspondence: wangxl0140@nuaa.edu.cn

Abstract

Ti6Al4V (TC4) titanium alloy is widely used in aerospace, biomedicine, and other high-precision applications due to its excellent specific strength, corrosion resistance, and biocompatibility. However, its surface quality directly affects the fatigue life and service performance of parts, and traditional polishing methods suffer from low efficiency and high pollution. As a non-contact, controllable surface treatment technology, nanosecond laser polishing has demonstrated unique advantages in balancing processing efficiency and surface quality. This study systematically discussed the influence of key process parameters (spot overlap rate, laser power, and scanning times) on nanosecond laser polishing of TC4 titanium alloy. It revealed the internal physical mechanism by analyzing the temperature and velocity fields and vortex dynamics during molten-pool evolution. It is found that the polishing effect is determined by the process parameters, which adjust the thermal-fluid coupling physical field (temperature distribution, melt flow, and vortex structure) in the molten pool. There is an optimal combination of parameters (spot overlap rate of 79%, laser power of 0.8W, scanning speed of 5m/min, scanning 3 times) that can place the molten pool in an optimal dynamic balance state and achieve effective flatness. The experimental results show that under this parameter, the surface roughness of the specimen with an initial roughness of 1.223 μm is reduced by about 32%. The research further clarified the mechanism by which the initial roughness of the base metal influences the molten pool: the greater the initial roughness, the more pronounced the "peak shaving and valley filling" effect. Under the same parameters, the improvement rate of the specimen with the initial roughness of 1.623 μm could reach about 40%. This study not only establishes the optimized process window, but also reveals the essential relationship between "process parameters - bath behavior - surface quality" from the level of the physical field of the molten pool, which provides an essential theoretical basis and practical guidance for the laser polishing process of TC4 titanium alloy high-precision surface.

Keywords: Ti6Al4V titanium alloy; nanosecond laser; surface roughness; polishing quality; physical mechanism

1. Introduction

Ti6Al4V (TC4) titanium alloy has high strength, good corrosion resistance, and excellent biocompatibility, and is widely used in aviation, aerospace, medical, and other fields [1]. However, the surface roughness of titanium alloy after additive manufacturing or machining will significantly reduce its fatigue life and tribological properties [2,3]. Therefore, it is necessary to study the polishing of TC4 specimens. Compared with traditional mechanical polishing and chemical polishing, laser polishing offers the advantages of non-contact operation, no tool wear, and greater controllability [4–6]. The thermal effect of nanosecond laser polishing is lower than that of long-pulse and CW lasers.

 doi:10.20944/preprints202602.0092.v1

Compared with the ultrashort pulse, the material removal efficiency is higher, thereby increasing polishing efficiency. Therefore, a nanosecond laser can be used for high-quality, efficient polishing of TC4 titanium alloy, which has low thermal conductivity [7–10].

Scholars at home and abroad have conducted extensive research on the physical mechanisms of laser polishing. Kumar et al. [11] used the line-focused beam and response surface method to study the laser polishing of 15-5 pH stainless steel produced by additive manufacturing. It was found that the mechanism was mainly based on superficial melting (SSM) and surface over melting (SOM), in which the surface tension drove the material to flow from peak to Valley to reduce the roughness; SSM is dominant at low energy density, while SOM is triggered at high energy density, resulting in increased shape error. Li et al. [12] achieved geometric smoothing and microstructure transformation by laser remelting at the edge of dual-phase steel. The mechanism involves transforming from a dual-phase (ferrite and martensite) state to pure martensite, eliminating microcracks and improving edge morphology. Hemwat et al. [13] discussed the mechanism of nanosecond laser polishing of 316L stainless steel, including the formation of a remelting layer, grain refinement, and atmosphere control (argon inhibiting oxidation) to promote the formation of a passive film, thereby improving corrosion resistance. In China, Li et al. [14] used continuous laser to polish TC4 under the condition of distributed heat source on the top cap, established a two-dimensional axisymmetric numerical transient model, simulated the evolution process of TC4 surface during the cooling process after laser heating to form the molten pool, and revealed the evolution mechanism of physical processes such as heat transfer, thermal radiation, thermal convection, melting and solidification involved in the polishing process. Among them, the capillary and thermal capillary mechanisms (Marangoni flow) play a key role in the smoothing process of the free-form surface of the molten pool. Pham et al. [15] revealed the synergistic effects of surface tension, recoil pressure, and Marangoni convection on the behavior of the molten pool during laser polishing through discrete element method and multiphysics computational fluid dynamics simulations. The simulation showed that when the energy density exceeded 0.3 J/mm, the recoil pressure enhanced polishing efficiency, whereas the initial surface roughness affected the flow stability of the molten pool. Li et al. [16] developed a two-dimensional transient numerical model to investigate the laser polishing mechanism of 3D-printed TC4 specimens. The results showed that a solidified surface structure with large roughness would be generated after high-power polishing, and the thermal capillary force dominated the formation process, driving the fluid to form tangential flow. However, low-power polishing results in a wavy structure with minor roughness. The appearance of this structure is mainly due to capillary force, which plays a dominant role in the molten pool flow, driving the melt to exhibit normal flow and thus eliminating the large surface curvature. Liu et al. [17] polished Cr12MoV die steel with a nanosecond pulse laser. By systematically adjusting the single-pulse energy density and beam overlap rate, it was found that when the energy density was 2.5 J/cm^2. The overlap rate was 95%, the surface roughness was the lowest (Sa 0.50 μm, reduced by 79.34%), and the mechanism study showed that the melting and gasification thresholds were 1.269 J/cm^2 and 2.937 J/cm^2, respectively. The molten pool was driven by surface tension to flow from the peak to the Valley (SSM mechanism), and excessive energy caused evaporation, resulting in surface ripples. Further, Liu et al. [18] established a computational fluid dynamics model to simulate the effect of evaporation pressure and Marangoni convection on the velocity field of the molten pool by coupling the fluid volume method. They found that a short pulse period can form a continuous molten pool that moves with the laser beam, making the surface along the scanning path tend to be flat. Under the influence of a large number of overlapping pulses, the SOM mechanism dominates the evolution of molten-pool morphology.

Studies at home and abroad have generally confirmed that the core of the laser polishing mechanism lies in the dynamic behavior of the molten pool. In foreign countries, most of them focus on the surface melting mechanism (SSM/SOM) and phase change regulation. In contrast, in China, the synergistic mechanism of capillary force and thermal capillary force on molten pool flow is further elucidated through high-precision numerical simulation, and the influence of the energy threshold on surface morphology is systematically quantified. However, the existing research on the

 doi:10.20944/preprints202602.0092.v1

mechanisms underlying the correlations among "process parameters, molten pool dynamics, surface quality" is limited, and the effect of initial surface morphology on polishing remains unclear.

In view of the above problems, this study aims to systematically elucidate the mechanism underlying the correlation between process parameters and surface quality by regulating the dynamic behavior of the molten pool during nanosecond laser polishing of TC4 titanium alloy. The innovative work is not only to establish the optimization window for key process parameters, but also to explain the polishing effect from the physical nature of the temperature and velocity fields and the vortex distribution in the molten pool, and to propose a process-matching strategy based on the initial roughness of the base metal. The research ideas are as follows: firstly, a two-dimensional transient numerical model of laser polishing is established based on the ablation principle, and the physical mechanism of polishing quality improvement is revealed through the temperature field, velocity field and eddy current distribution in the molten pool; Then, the influence of spot overlap rate, laser power and scanning times on surface roughness was explored by single factor experiment, and the optimal parameter combination was determined; Secondly, combined with the physical field of molten pool evolution, the internal mechanism of the influence of various parameters on the polishing quality is analyzed; Finally, the impact of the initial roughness of the base metal on the polishing effect is investigated, and the corresponding parameter selection principle is established. To provide theoretical and technological guidance for the realization of high-quality and efficient polishing of the TC4 titanium alloy surface.

2. Mathematical Modeling

2.1. Physical Model and Assumptions

Nanosecond laser polishing improves the surface quality of the workpiece through surface remelting [19]. When the laser beam irradiates the upper surface of the workpiece, its temperature will quickly reach the melting point, forming a molten pool and a heat-affected zone (HAZ). The molten pool will move along the laser scanning direction (Figure 1a). To study the evolution mechanism of the rough surface in the above laser polishing process, considering heat transfer, laminar flow, gravity, recoil pressure, surface tension and Marangoni effect, the level set method is used to track the geometry of the gas/liquid interface, and a two-dimensional model of transient multi physical field coupling is established (Figure 1b). The size of the polishing layer is 2000 μm × 1500 μm. The dimensions of the protective argon gas layer are 2000 μm × 500 μm. The upper surface of the polished layer is a random rough surface, and the laser scans along the X-axis. The physical properties and process parameters of the materials used in the simulation are shown in Table 1.

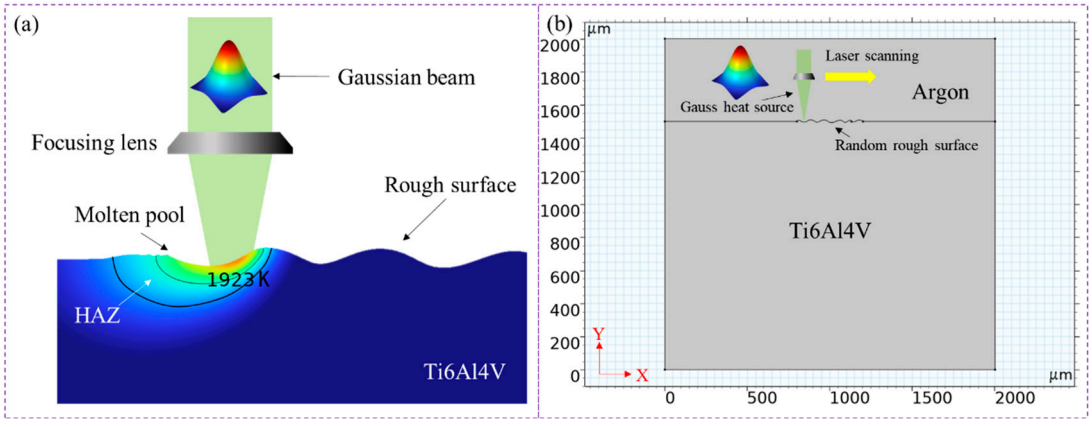

Figure 1. Schematic diagram and model representation of laser polishing.

 doi:10.20944/preprints202602.0092.v1

Table 1. Thermo-physical properties of Ti6Al4V and process parameters [20].

Physical Property (Units)	Symbol	Value
Solid density (kg/m³)	ρ_s	4520
Liquid density (kg/m³)	ρ_l	4210
Air density (kg/m³)	ρ_{air}	0.5
Solid thermal conductivity (W/(m·K))	k_s	21
Liquid thermal conductivity (W/(m·K))	k_l	30
Air thermal conductivity (W/(m·K))	k_{air}	0.07
Specific heat (J/(kg·K))	C_m	700
Air specific heat (J/(kg·K))	C_{air}	520
Latent heat of fusion (J/kg)	L_m	3.896×10^5
Latent heat of vaporization (J/kg)	L_v	9.462×10^6
Room temperature (K)	T_0	293.15
Solidus temperature (K)	T_s	1877
Liquidus temperature (K)	T_l	1923
Melting temperature (K)	T_m	1903
Evaporating temperature (K)	T_v	3315
Convective coefficient (W/(m²·K))	h_0	30
Ambient pressure (atm)	P_0	1
Surface tension coefficient (N/m)	γ	$1.65\text{-}0.28\times10^{-3}T$
Solid dynamic viscosity (Pa·s)	μ_s	100
Liquid dynamic viscosity (Pa·s)	μ_l	0.005
Air dynamic viscosity (Pa·s)	μ_{air}	1×10^{-4}
Power density (GW/m²)	P_d	48
Spot radius (μm)	r_0	50
Scanning speed (m/s)	V_{laser}	0.75

To simplify the numerical calculation, assume the following [19]:

(1) Due to the short interval between laser pulses, the pulsed laser heat source is regarded as a continuous Gaussian heat source.

(2) The effect of deformation on the fluid field is ignored.

(3) The laser absorptivity of the material is constant.

(4) The flow field in the molten pool is incompressible Newtonian laminar flow.

(5) The material is isotropic and homogeneous.

(6) Ignore metal loss due to evaporation.

2.2. Governing Equations and Boundary Conditions

As shown in Figure 1b, the rough surface is irradiated by Gaussian laser heat flow, and considering the convection effect on the environment, its heat transfer equation follows the Fourier law [19]:

$$\rho C_m\left(\frac{\partial T}{\partial t}+\vec{u}\cdot\nabla T\right)=\nabla\cdot\left(k\nabla T\right)+Q \quad (1)$$

Where ρ is the density, C_m is the specific heat capacity, T is the temperature, t is the time, $\vec{u}$ is the fluid flow rate, k is the thermal conductivity, and Q is the heat transfer term.

Thermal convection can be expressed as [14]:

 doi:10.20944/preprints202602.0092.v1

$$-k\nabla T = h_0\left(T_0 - T\right) \quad (2)$$

Where h_0 is the convection coefficient, and T_0 is the room temperature.

The flow field in the molten pool can be calculated by the Navier-Stokes equation [16]:

$$\rho\frac{\partial\vec{u}}{\partial t} + \rho\left(\vec{u}\cdot\nabla\vec{u}\right) = \nabla\cdot\left(-p\vec{I} + \mu\left(\nabla\vec{u} + \nabla^T\vec{u}\right)\right) + \vec{F} \quad (3)$$

Where μ is the dynamic viscosity, $\vec{I}$ is the identity matrix, p is the fluid pressure, and $\vec{F}$ is the source term related to surface tension, gravity, and Marangoni force.

The laser heat flux Q_{laser} for rough surface polishing is [19]:

$$Q_{laser} = 2P_d\exp\left(\frac{-2\left(x - x_0 - V_{laser}\cdot t\right)^2}{r_0^2}\right) \quad (4)$$

Where P_d is the laser power density, r_0 is the spot radius, x_0 is the initial beam position, and V_{laser} is the laser scanning speed.

Considering the Marangoni effect and the influence of thermal gradient on the molten pool, the surface tension $\vec{\sigma}$ can be expressed as [19]:

$$\vec{\sigma} = \kappa\gamma\cdot\vec{n} + \nabla_s\gamma \quad (5)$$

Where κ is the curvature, γ is the surface tension coefficient, $\vec{n}$ is the surface normal vector, ∇_s is the surface gradient operator, and$\nabla_s\gamma$ is the Marangoni effect caused by the temperature gradient.

When the temperature of the upper surface rises to the boiling point, the evaporated metal vapor will generate a recoil pressure P_r, which can be expressed as [19]:

$$P_r = 0.54P_0\exp\left(L_v\left(\frac{T - T_v}{RTT_v}\right)\right) \quad (6)$$

Where P_0 is the ambient pressure, L_v is the latent heat of evaporation, R is the universal gas constant, and T_v is the evaporation temperature.

2.3. Numerical Simulation Results and Discussions

The evolution of molten pool morphology during laser polishing of TC4 titanium alloy is shown in Figure 2. The figure shows that the molten pool forms rapidly (0.15ms) under the laser's action and expands over time (0.30ms, 0.40ms). Its shape and temperature gradient (decreasing outward from the core high-temperature zone) directly affect the viscosity and flow-driving force of the molten metal. It provides a physical image of how laser energy density (determined by power and spot overlap rate) controls the size and duration of the molten pool. Further, the streamline diagram shows strong convection in the molten pool, especially in the vortex-forming area marked in the blue box in the figure. This vortex flow is the primary mechanism for energy and mass transfer in the molten pool. It can effectively transport molten material from the bulge (high temperature, low surface tension) to the depression (low temperature, high surface tension), thereby achieving the "leveling" effect on the surface, which is the core physical mechanism of polishing. Moreover, from 0.15ms to 0.40ms, it can be observed that the vortex structure is clear and stable throughout emergence and development. At 0.60ms, the vortex morphology further evolves, and the structure may become more complex due to flow development, energy dissipation, or multi-vortex interaction. It indicates that there is an "optimal action time window" in the polishing process. During this period, the fully developed and stable vortex can most effectively promote material homogenization, and the process parameters (such as the scanning speed and frequency that affect the spot overlap rate) must be matched to take advantage of this window.

 doi:10.20944/preprints202602.0092.v1

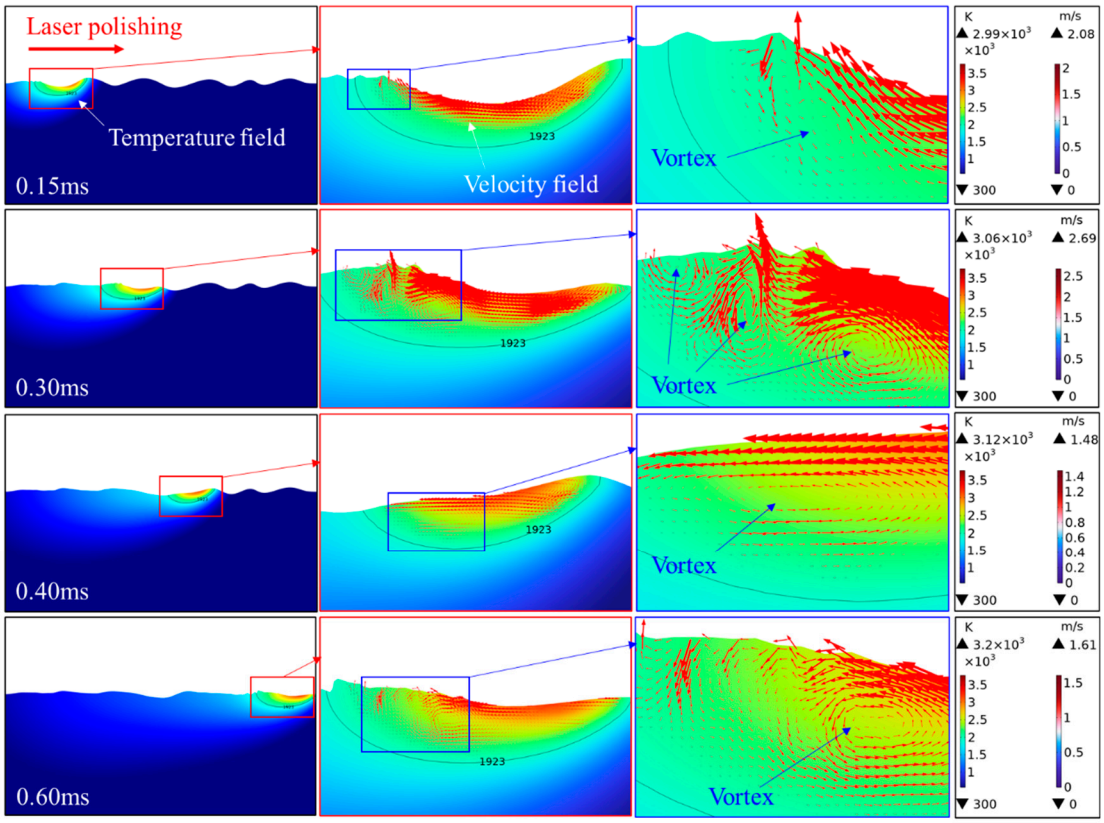

Figure 2. Evolution of molten pool morphology during laser polishing of TC4 titanium alloy: temperature field, velocity field, and vortex distribution.

In summary, the real-time coupling among the temperature field (driving force source), the velocity field (material response), and the vortex (flow core structure) is revealed. Specifically, the high-temperature region drives a strong surface-tension gradient (Marangoni effect), which induces melt flow and vortex formation; conversely, flow affects the transmission and distribution of heat. It constitutes a complete closed loop of "energy input - thermal drive - flow response - morphology change", which provides a full and dynamic physical framework for explaining how subsequent changes in process parameters ultimately affect the surface quality through the coupling system of disturbance.

3. Experimental Equipment and Methods

3.1. Preparation of Materials

The polishing material used in the experiment is TC4 titanium alloy. EDM prepares a 50mm × 50mm × 10mm test piece, and its chemical composition is shown in Table 2. The root-mean-square height (Sq) of the surface was measured using a three-dimensional profilometer, and the average of six areas from each specimen was taken as the initial roughness. To study the influence of the initial roughness of the base metal, the test pieces (test pieces 1-4) with different initial surface states were prepared in the experiment. The initial roughnesses were 1.013 μm, 1.623 μm, 1.035 μm, and 1.223 μm, respectively. The surface morphology is shown in Figures 3 and 4.

Table 2. Main chemical composition of Ti6Al4V (wt%) [14].

Ti	Al	V	C	Fe	O	N
Balance	5.50-6.75	3.50-4.50	0.08	0.30	0.20	0.05

 doi:10.20944/preprints202602.0092.v1

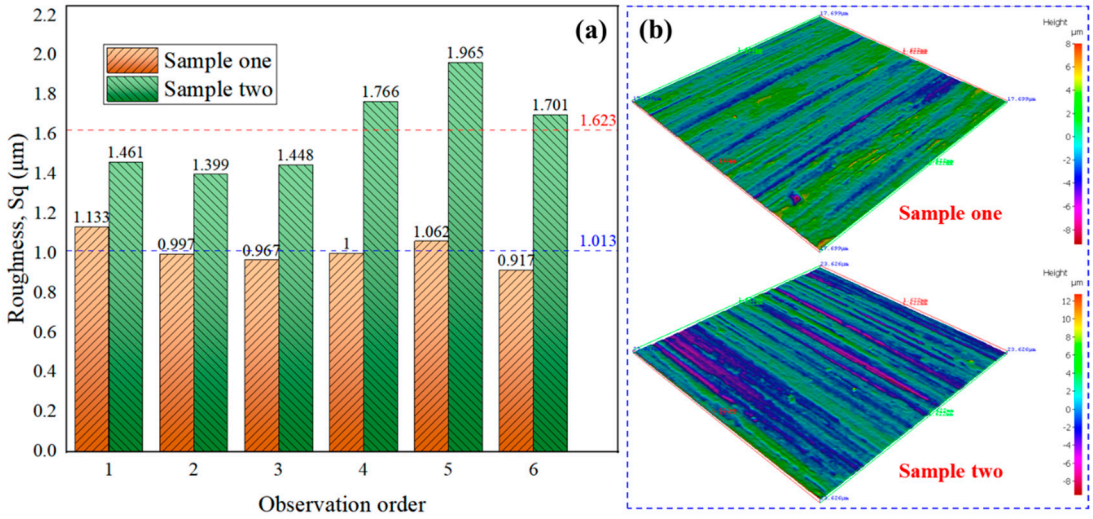

Figure 3. Initial surface roughness and morphology of specimens 1 and 2.

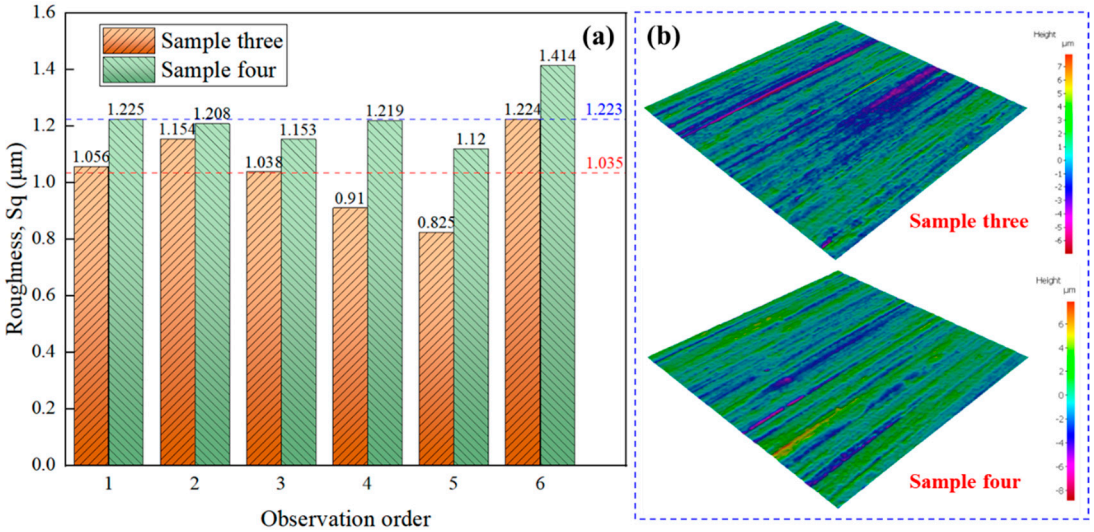

Figure 4. Initial surface roughness and morphology of specimens 3 and 4.

3.2. Nanosecond Laser Polishing System

In the experiment, a fiber nanosecond laser (wavelength 532nm, pulse width 15 ns) was used to achieve accurate scanning path control on the X-Y workbench (Figure 5a). The spot diameter was 40 μm. The scanning strategy adopted the equal-overlap-rate progressive scanning mode, as shown in Figure 5b. The specific spot overlap rate was controlled by adjusting the pulse repetition rate (F) and the scanning speed (V). Spot overlap rate (ξ) is the core parameter of polishing, and its calculation formula is as follows:

$$\xi = \frac{\Delta x}{D} = \frac{\Delta y}{D} \approx 1 - \frac{V}{F \cdot D} \quad (7)$$

Where D is the spot diameter, and Δx and Δy are the overlapping length in the scanning direction and spacing direction, respectively.

 doi:10.20944/preprints202602.0092.v1

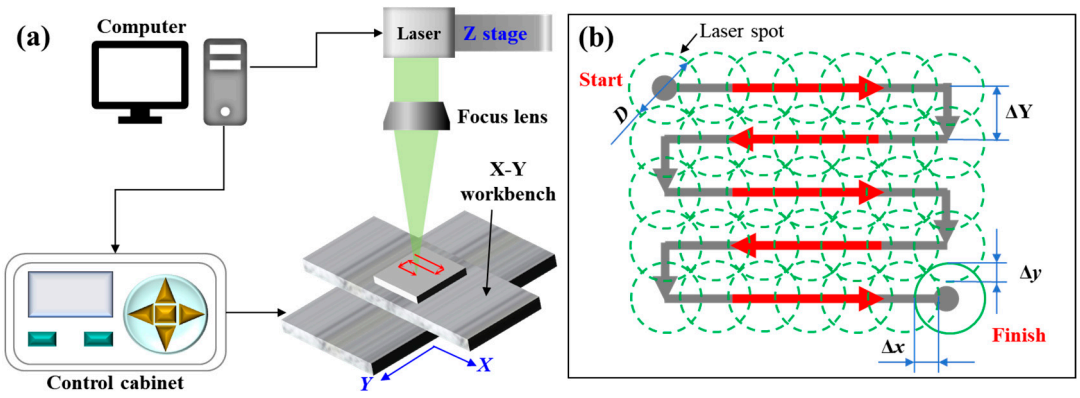

Figure 5. Laser polishing system and its scanning strategy.

3.3. Experimental Design

The effects of spot overlap rate (60%-85%), laser power (0.8-3.8W), and scanning times (1-4) on polishing quality were studied by the univariate method. After polishing, all specimens were ultrasonically cleaned in clean water for 30 minutes to remove surface residues. To ensure statistical reliability, the polishing area under each parameter is randomly measured 4 times, and the average is used as the final roughness of the region. The surface roughness change rate (ΔSq) is used to quantify the polishing effect, and the calculation formula is:

$$\Delta Sq=\frac{Sq_{av}-Sq_0}{Sq_0}\times 100 \quad (8)$$

Where Sq_0 is the initial surface roughness, and Sq_{av} is the average surface roughness after polishing. A negative ΔSq indicates that roughness is reduced.

4. Results and Discussion

4.1. Influence of Spot Overlap Rate on Laser Polishing

When the laser power (*P*) is 2.7W, the scanning speed is 5m/min, and the scanning times is 1 (according to the previous experimental exploration, the processing quality is good under this parameter, and the processing depth is equivalent to the original roughness of TC4), the influence of the spot overlap rate (achieved by changing the pulse repetition rate) on the polishing quality is studied. The specific parameters are shown in Table 3.

Table 3. Process parameters of spot overlap rate on nanosecond laser polishing quality of TC4.

Parameters	Values
P (W)	2.7
V (m/min)	5
F (kHz)	5.2, 6, 7, 8.3, 10, 14
ξ (%)	60, 65, 70, 75, 79, 85

As the overlap rate of the light spot increases from 60% to 79%, the surface roughness decreases, and the best polishing effect is achieved at 79%. The roughness is reduced by 14.911% (as shown in Figure 6a). This can be further explained from the perspective of the physical field of molten pool evolution (Figure 2): appropriately increasing the spot overlap rate (to 79%) means that the adjacent laser pulses are more closely connected in time and space. As shown in Figure 2, at different times during laser action (0.15ms-0.60ms), the molten pool undergoes formation, expansion, and the

 doi:10.20944/preprints202602.0092.v1

development of an internal flow field (including a vortex). The higher overlap rate helps to input the energy of the subsequent pulse when the molten pool formed by the previous pulse is not fully solidified. This connection can maintain a relatively stable, extended melting state, allowing Marangoni convection driven by a temperature gradient to have more time for material transport, thus more effectively realizing "peak shaving and valley filling" and surface leveling [11]. At the same time, moderate superposition of heat inputs also promotes a more gentle spatial temperature gradient, reducing residual stress and microfluctuations caused by rapid cooling [17]. However, when the overlap rate continues to increase to 85%, the too short pulse interval will lead to the continuous and excessive accumulation of heat in the action area, which may lead to the high temperature of the molten pool, intensified evaporation, instability of the melt flow (velocity field), increased spatter, and even damage to the flattened surface, which will reduce the surface quality (as shown in Figure 6b, the surface is rough when the overlap rate is 85%) [18].

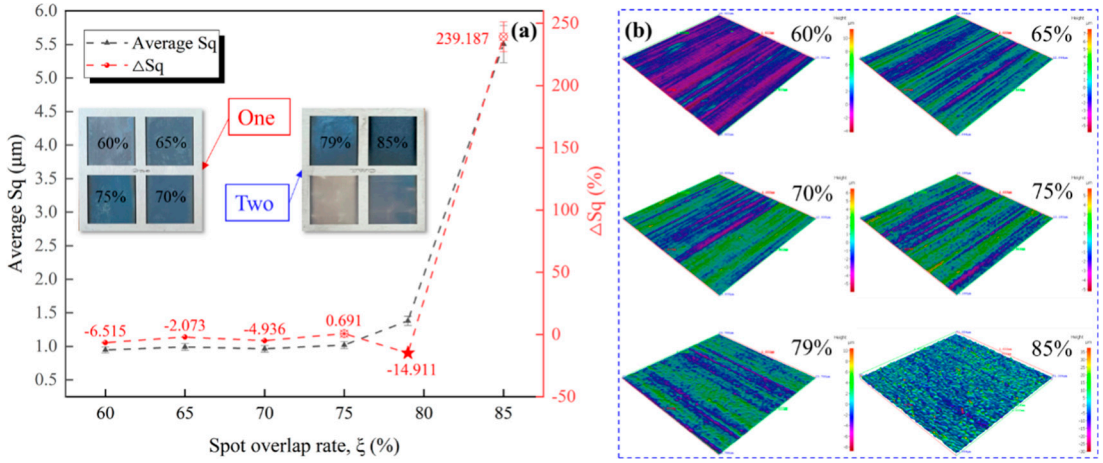

Figure 6. Effect of spot overlap rate on surface roughness and surface morphology.

4.2. Influence of Laser Power on Laser Polishing

Based on the conclusion in 4.1, the influence of laser power is studied under the conditions of an optimal spot overlap rate of 79%, a scanning speed of 5m/min, and a scanning times of 1. The specific parameters are shown in Table 4.

Table 4. Process parameters of laser power on the nanosecond laser polishing quality of TC4.

Parameters	Values
P (W)	0.8, 1.4, 1.9, 2.7, 3.4, 3.8
V (m/min)	5
F (kHz)	10
ξ (%)	79

With the increase of laser power from 0.8W to 3.8W, the polishing effect improved first and then deteriorated. The best effect was obtained at 0.8W, and the roughness was reduced by 39.988% (Figure 7a). Combined with the analysis of the physical field of the molten pool (Figure 2), its internal mechanism is that the laser power directly controls the energy input intensity of the molten pool, which determines the core characteristics of the temperature field, velocity field and vortex evolution, and then dominates the surface forming quality. Specifically, at low power (such as below 0.8W), insufficient energy input leads to low bath temperature, high melt viscosity, and weak melt flow driven by temperature gradient (Marangoni effect). This makes it difficult for the molten material to

 doi:10.20944/preprints202602.0092.v1

flow and redistribute fully, and it is impossible to effectively implement "peak shaving and valley filling" [11,16]. At the optimal power of 0.8W, the energy input and thermal diffusion reach an ideal balance. At this time, the molten pool can form characteristics with a significant temperature gradient and an appropriate size, as shown in Figure 2. The strong temperature gradient drives fully developed melt convection and forms a clear, stable vortex structure during the 0.30-0.40 ms stage. The vortex can efficiently promote the mixing and transport of materials in the molten pool, thereby carrying the molten material from the micro bulge to the depression and achieving a significant smooth effect. When the power is too high (e.g., up to 3.8W), the excessive energy input leads to a sharp rise in the core temperature of the molten pool (the high-temperature region in the temperature field is significantly expanded, and the temperature value is far beyond the melting boiling point of the material), causing severe material evaporation. The recoil pressure generated by evaporation will seriously disturb, or even destroy, the original orderly flow-field structure in the molten pool (which may lead to velocity-field disorder and vortex instability) and induce melt splashing [16]. As a result, the material is selectively removed rather than redistributed, and new pits, spheroidization, and heavy condensates are readily accumulated on the surface, thereby deteriorating surface quality (Figure 7b).

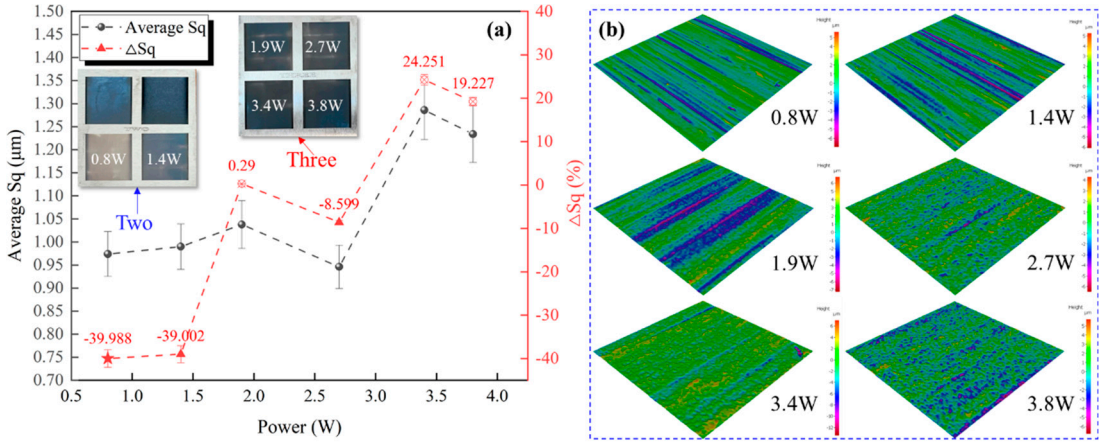

Figure 7. Effect of laser power on surface roughness and surface morphology.

4.3. Influence of Scanning Times on Laser Polishing

Based on the optimal parameters (spot overlap rate 79%, laser power 0.8W, scanning speed 5m/min), the influence of scanning times N (1 to 4) is studied. The specific parameters are shown in Table 5.

Table 5. Process parameters of scanning times on the nanosecond laser polishing quality of TC4.

Parameters	Values
P (W)	0.8
V (m/min)	5
F (kHz)	10
ξ (%)	79
N	1, 2, 3, 4

Over the range of scanning times (1-4), the surface roughness decreased, and the best polishing effect was obtained with 3 scans, with roughness reduced by 31.889% (Figure 8a). Combined with the analysis of the dynamic evolution of the molten pool's physical field (Figure 2), the influence

 doi:10.20944/preprints202602.0092.v1

mechanism of the scanning times lies in their repeated regulation of the "heat flow solidification" cycle in the same action area. Specifically, the initial molten pool was formed on the original rough surface in the first scan, which experienced the complete evolution of the physical field as shown in Figure 2: the temperature field was established and driven to flow, the melt was redistributed under the action of convection and vortex (as shown in the 0.30ms-0.40ms stage) and solidified, forming a initially flat but micro undulating melt layer. Moderate follow-up scanning (2-3 times) acts on the melted layer. Its key role is "iterative trimming": the energy input by the follow-up laser not only melts the residual micro bulges again, but also induces the formation of a new molten pool (the evolution of the physical field is similar to that in Figure 2, but based on a smoother initial morphology) that can carry out secondary or tertiary leveling for the remaining fine unevenness after the previous solidification, to improve the overall flatness cumulatively [15]. However, when the scanning times are too many (e.g., 4), the same area undergoes multiple high-temperature thermal cycles, resulting in continuous heat accumulation (similar to the high-temperature area in Figure 2 being repeatedly and superimposed). This excessive heat input will keep the bath temperature excessively high, which may not only cause excessive evaporation and splashing of materials but also make the melt flow (velocity field) unstable due to overheating, and even destroy the favorable leveling structure formed in the previous scan [18]. As a result, the excessive "heat flow" disturbance replaces the ordered "iterative trimming", leading to a decrease in surface quality (Figure 8b).

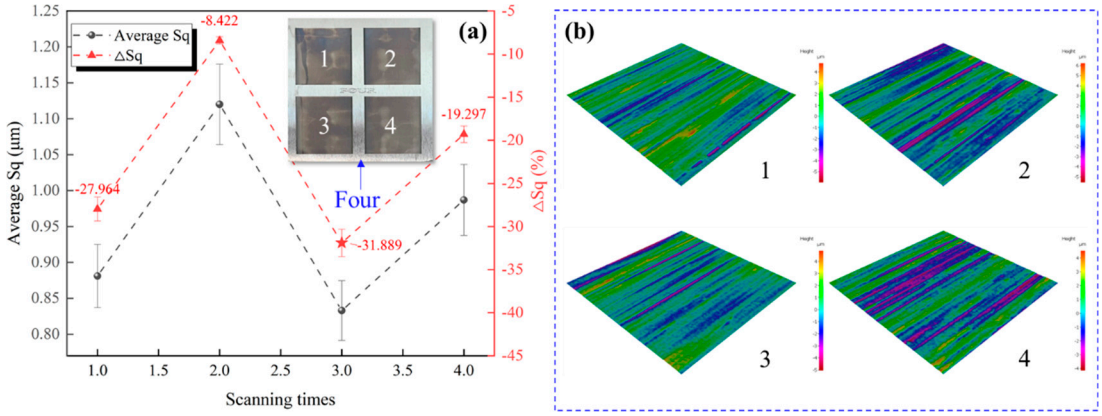

Figure 8. Effect of scanning times on surface roughness and surface morphology.

4.4. Effect of Initial Roughness of Base Metal

Comprehensive analysis of the data in Table 6 shows that, under the same polishing parameters, the reduction in the absolute value of roughness (|△Sq|) of the base metal with a larger initial roughness (such as test piece 2, Sq=1.623 μm) after polishing is usually greater. It shows that nanosecond laser polishing has a more significant effect on improving the surface in a poor initial state. Based on the in-depth analysis of the molten pool's physical field behavior (Figure 2), the fundamental reason is that different initial shapes exhibit distinct responses to the "energy flow morphology" coupling mechanism. For the surface with large initial roughness, its significant macro peak valley structure will produce a highly non-uniform temperature field under the action of the laser: the convex peak absorbs more energy, reaches the melting temperature faster, and forms a molten pool, while the concave valley is relatively less heated [15]. As shown in Figure 2, once the molten pool forms, the strong temperature gradient drives Marangoni convection, and the resulting vortex structure efficiently carries molten material from the high-temperature convex area to the low-temperature concave area. Due to the large initial fluctuation, the material transport amplitude during "peak shaving and valley filling" is large, and the efficiency is high, resulting in a significant improvement in the absolute value of roughness. On the contrary, for the initially smooth surface, its micro-fluctuation scale is small, the temperature distribution within the molten pool coverage is relatively uniform, and the dynamic and spatial requirements of melt flow and material

 doi:10.20944/preprints202602.0092.v1

redistribution driven by the temperature gradient are minor [15]. Therefore, the "leveling" correction range of morphology achieved by a single scan is limited, and the absolute reduction in roughness is also slight. At this time, as described in Section 4.3, the micro morphology can be further optimized by appropriately increasing the number of scans and using the "iterative dressing" effect of subsequent laser action on the preliminarily flattened surface to induce new and finer molten pool flow, but this is based on the premise of controlling heat accumulation and avoiding damage.

Table 6. Influence of base material roughness on the nanosecond laser polishing quality of TC4.

Base material	Processing parameters	Average Sq (μm)	|ΔSq| (%)
Two	79%、2.7W、5m/min、1	1.381	14.911
Three		0.946	8.599
Two	79%、0.8W、5m/min、1	0.974	39.988
Four		0.881	27.964

5. Conclusions

(1) The process parameters jointly determine the polishing quality by adjusting the physical field of the molten pool: the influence of spot overlap rate, laser power and scanning times on the quality of nanosecond laser polishing of TC4 titanium alloy, whose internal physical essence is to control the dynamic evolution process of the laser-induced molten pool, including the distribution of temperature field, the morphology and stability of melt flow (especially the vortex structure), and the final solidification behavior. In this study, the optimal parameter combination (spot overlap rate 79%, laser power 0.8W, scanning speed 5m/min, scanning times 3) was obtained, which makes the molten pool in the "energy input thermal diffusion" equilibrium state, to form a stable size, sufficient convection (vortex development well) and controllable heat accumulation of the molten pool, and ultimately achieve the best polishing effect.

(2) The optimization window of laser power corresponds to the critical transition between the stable level of the molten pool and the excessive evaporation state: when the power is too low, the energy input is insufficient, the molten pool temperature and melt fluidity (velocity field strength) are limited, and the material cannot be fully melted and flowing; When the power is too high, the excessive energy input causes the core temperature of the molten pool to rise sharply, causing severe evaporation and recoil pressure, destroying the stability of the molten pool flow field and inducing splashing. Therefore, the best polishing effect corresponds to a power window that allows the molten pool to flow in a sufficient and orderly manner (especially a stable vortex transport) without causing excessive evaporation.

(3) The initial roughness of the base metal determines the action range and process strategy of "peak and valley cutting" in the molten pool: under the same process parameters, the significant peak and valley structure of the surface with larger initial roughness will produce stronger temperature gradient and non-uniform melting under the action of laser, thus driving more intense melt flow and material transport, so the absolute value of roughness will be reduced more significantly. For the initial smooth surface, the correction of microfluctuations depends more on the multiple "melting leveling" iterative dressing effect induced by the moderate increase in scanning times, but heat accumulation should be strictly controlled.

(4) Through the combination of process experiments and physical field analysis of the molten pool, this study systematically revealed the internal mechanism between "process parameters - molten pool physical field (temperature field/velocity field/vortex) - surface morphology". It clarified the physical mechanism by which each parameter ultimately determines polishing quality by affecting the thermodynamic and hydrodynamic behavior of the molten pool, providing a solid theoretical basis for the precise process design and optimization of nanosecond laser polishing of TC4 titanium alloy.

Author Contributions: Conceptualization, X.W.; investigation, X.W. and J.M.; writing—original draft preparation, X.W.; writing—review and editing, J.M. All authors have read and agreed to the published version of the manuscript.

Funding: This research was funded by [Jiangsu Provincial Natural Science Foundation Youth Science Fund] grant number [BK20241404].

Data Availability Statement: All data relevant to this study are provided within the paper.

Conflicts of Interest: The authors declare no conflicts of interest.

References

1. Song, Y.Y.; Zhou, J. Experimental study on multi-laser asynchronous polishing of TC4 titanium alloy by laser metal deposition additive manufacturing. *Surface Technology* **2025**, *54*, 174-182. [DOI:10.16490/j.cnki.issn.1001-3660.2025.17.015]
2. Zhang, X.J.; Tang, S.Y.; Zhao, H.Y.; Guo, S.Q.; Li, N.; Sun, B.B.; Chen, B.Q. Research status and key technologies of 3D printing. *Journal of Materials Engineering* **2016**, *44*, 122-128. [DOI:10.11868/j.issn.1001-4381.2016.02.019]
3. Hou, Y.K.; Yuan, J.T.; Wang, Z.H.; Wang, B.X. Milling parameters optimization and analysis of selective laser melted Ti6Al4V. *Manufacturing Technology and Machine Tool* **2016**, *1*, 103-107. [DOI:10.19287/j.cnki.1005-2402.2016.01.028]
4. Chen, B.W.; Sun, S.F.; Wang, X.; Zhang, F.Y.; Shao, Y.; Zhang, L.L.; Zhao, D.L.; Wang, P.P.; Chen, X.Z.; Liu, J.X.; Cao, A.X.; Sun, W.L. Research progress of laser polishing technology for material surface. *China Surface Engineering* **2021**, *34*, 74-89. [DOI:10.11933/j.issn.1007-9289.20210702001]
5. Dai, W.; Zheng, Z.Z.; Li, J.J.; Huang, Q.W.; Liu, J. Research progress of laser polishing on the metal surface. *Laser Optoelectronics Progress* **2015**, *52*, 110001. [DOI:10.3788/LOP52.110001]
6. Song, Y.; Wang, H.P.; Wang, Q.; Ma, C.P.; Guan, Y.C. Research and application of laser fine surface processing technology: cleaning and polishing. *Aeronautical Manufacturing Technology* **2018**, *61*, 78-86. [DOI:10.16080/j.issn1671-833x.2018.20.078]
7. Wang, X.L.; Ma, J.W.; Jia, Z.Y.; Gui, C.H.; Qi, X.Q.; Liu, W. Nanosecond laser high-precision fabrication of microgrooves on TC4 surface: Morphology simulation and drag reduction performance of microgrooves. *J. Laser Appl.* **2022**, *34*, 042047. [DOI:10.2351/7.0000745]
8. Wang, X.L.; Jia, Z.Y.; Ma, J.W.; Han, D.X.; Gui, C.H.; Qi, X.Q.; Liu, W. Research on nanosecond laser processing of basic unit for ridge surface: forming condition of microgroove and micro-ridge structure on TC4 surface. *Opt. Eng.* **2022**, *61*, 046105. [DOI:10.1117/1.OE.61.4.046105]
9. Wang, X.L.; Jia, Z.Y.; Ma, J.W.; Han, D.X.; Qi, X.Q.; Gui, C.H.; Liu, W. Optimization of nanosecond laser processing for microgroove on TC4 surface by combining response surface method and genetic algorithm. *Opt. Eng.* **2022**, *61*, 086103. [DOI:10.1117/1.OE.61.8.086103]
10. Wang, X.L.; Jia, Z.Y.; Ma, J.W.; Liu, W.; Han, D.X.; Gui, C.H.; Qi, X.Q. Research on simulation of nanosecond pulsed laser processing for TC4 titanium alloy: A novel model simplification and correction method. *Opt. Laser Technol.* **2022**, *147*, 107635. [DOI:10.1016/j.optlastec.2021.107635]
11. Kumar, A.; Ramadas, H.; Kumar, C.S.; Nath, A.K. Laser polishing of additive manufactured stainless-steel parts by line focused beam: A response surface method for improving surface finish. *J. Manuf. Process.* **2025**, *133*, 1310-1328. [DOI:10.1016/j.jmapro.2024.12.028]
12. Li, D.; Linnenbrink, S.; Tekkaya, B.; Dölz, M.; Willenborg, E.; Könemann, M.; Münstermann, S. Optimizing sheet metal edge quality with laser-polishing: surface characterization and performance evaluation. *Int. J. Mater. Form.* **2024**, *17*, 48. [DOI: 10.1007/s12289-024-01847-7]
13. Hemwat, J.; Saetang, V.; Qi, H.; Seenawat, M.; Chankitmunkong, S.; Pandee, P. Laser surface polishing of material extrusion additively manufactured 316L stainless steel. *Opt. Laser Technol.* **2026**, *194*, 114442. [DOI: 10.1016/j.optlastec.2025.114442]
14. Li, K.; Zhao, Z.Y.; Zhou, H.M.; Zhou, H.; Jin, J.C. Numerical analyses of molten pool evolution in laser polishing Ti6Al4V. *J. Manuf. Process.* **2020**, *58*, 574-584. [DOI:10.1016/j.jmapro.2020.08.045]

 doi:10.20944/preprints202602.0092.v1

15. Pham, D.; Tran, H.C. Multi-physics simulation for predicting surface roughness of laser powder bed fused parts after laser polishing. *Addit. Manuf.* **2024**, *94*, 104486. [DOI:10.1016/j.addma.2024.104486]
16. Li, J.J.; Wu, H.Y.; Liu, H.X.; Zuo, D.W. The effect of molten pool evolution on the formation of surface structures during laser polishing. *Precis. Eng.* **2024**, *86*, 170-182. [DOI:10.1016/j.precisioneng.2023.12.001]
17. Liu, Z.H.; Wang, C.M.; Mi, G.Y.; Zhang, W.; Wang, J. Surface morphological evolution and microhardness change of Cr12MoV steel by pulsed laser polishing. *Opt. Laser Technol.* **2024**, 171, 110419. [DOI:10.1016/j.optlastec.2023.110419]
18. Liu, Z.H.; Hu, Y.Y.; Zhang, M.Y.; Zhang, W.; Wang, J.; Lei, W.B.; Wang, C.M. Surface morphology evolution mechanisms of pulse laser polishing mold steel. *Int. J. Mech. Sci.* **2024**, *269*, 109039. [DOI:10.1016/j.ijmecsci.2024.109039]
19. Zhou, J.T.; Han, X.; Li, H.; Liu, S.; Shen, S.N.; Zhou, X.; Zhang, D.Q. In-situ laser polishing additive manufactured AlSi10Mg: Effect of laser polishing strategy on surface morphology, roughness and microhardness. *Materials* **2021**, *14*, 393. [DOI:10.3390/ma14020393]
20. Li, H.; Shen, S.N. Application of finite element software COMSOL Multiphysics in Engineering. Science Press: Beijing, China, 2023, 83-115.